The Astrophysical Journal, 581:1194–1203, 2002 December 20

STAR FORMATION IN SPACE AND TIME: TAURUS-AURIGA

Francesco Palla[1] and Steven W. Stahler[2]
Received 2002 April 10; accepted 2002 August 21

ABSTRACT

To understand the formation of stellar groups, one must first document carefully the birth pattern within real clusters and associations. In this study of Taurus-Auriga, we combine pre–main-sequence ages from our own evolutionary tracks with stellar positions from observational surveys. Aided by the extensive millimeter data on the molecular clouds, we develop a picture of the region's history. Star formation began, at a relatively low level and in a spatially diffuse manner, at least 10^7 yr in the past. Within the last few million years, new stars have been produced at an accelerating rate, almost exclusively within a confined group of striated cloud filaments. The gas both inside and around the filaments appears to be in force balance. Thus, the appearance of the filaments is due to global, quasi-static contraction of the parent cloud material. Gravity drives this contraction and shock dissipation mediates it, but the internal motion of the gas does not appear to be turbulent. The accelerating nature of recent star formation means that the condensation of cloud cores is a threshold phenomenon, requiring a minimum background density. Other, nearby cloud regions, including Lupus and Chamaeleon, contain some locales that have attained this density, and others that have not. In the latter, we find extensive and sometimes massive molecular gas that is still devoid of young stars.

Subject headings: ISM: clouds — ISM: individual (Taurus-Auriga) — ISM: kinematics and dynamics — open clusters and associations: general — stars: formation — stars: pre–main-sequence

1. INTRODUCTION

One basic characteristic of stars is that they form not as isolated objects, but in populous groups within molecular clouds and cloud complexes. This observational fact raises other basic issues of a theoretical nature. What supports a massive cloud against its self-gravity *before* the production of an interior stellar group? How do individual dense cores, each capable of forming single and binary stars, arise within this kinetic, and perhaps turbulent, medium? Which properties of the large parent cloud determine whether it will spawn a bound cluster, T association, or expanding OB association?

Answering all these questions will require a broader and deeper understanding than is currently at hand, one that connects the birth of individual stars to the growth and evolution of clouds on a multiparsec scale. Any such theory, if it is to be quantitative, must be based on detailed information concerning the earliest stages of existing groups. That is, we should first ascertain the actual pattern of stellar births in observed clusters and associations. To address this issue, we began by constructing a set of pre–main-sequence evolutionary tracks (Palla & Stahler 1999; hereafter Paper I). These covered masses from 0.1 to 8 $M_\odot$, i.e., from close to the brown dwarf regime to the upper mass limit of the pre–main-sequence phase itself (Palla & Stahler 1990). The tracks can be used to assign contraction ages to any young star that has reliable values of effective temperature and luminosity. A compilation of ages then represents the star formation history of the region of interest.

Paper I applied this method to the Orion Nebula cluster. Utilizing the extensive database of Hillenbrand (1997), we found that star formation began at a relatively low rate at least 10^7 yr ago, then increased markedly within the last 2×10^6 yr. In a subsequent contribution (Palla & Stahler 2000; hereafter Paper II), we examined seven additional, nearby groups. Most exhibited a similar pattern of activity as Orion: a slow rise followed by rapid acceleration through the current epoch.

This result has recently been questioned by Hartmann (2001), who claims that observational errors in effective temperatures and luminosities are so large that they preclude the inference of any detailed history at all. Hartmann further contends that the data from T associations are consistent with a rapid burst of star formation in the recent past, and that apparently older stars have simply been assigned erroneously low luminosities. This view is contradicted, however, by the H-R diagrams in Papers I and II. If the observational errors were indeed large enough to "age" a substantial portion of stars, they would also give spuriously *high* luminosities to an equal number of other objects. Many of these would appear above the birth line in the H-R diagram, which is not the case. In his statistical analysis, Hartmann avoids this difficulty by ignoring the birth line and allowing arbitrarily high luminosities for his sample population (see his eq. [2] and Fig. 2).

Assuming that our findings are robust, many systems are increasing their production of stars to the present time. This intriguing result naturally prompts additional questions. Where are the clouds that are not yet actively forming stars? Within a given cloud, what ends the acceleration?

A partial answer to the second point is available from the earlier studies. In the volume surveyed by Hillenbrand (1997), i.e., within several parsecs of the Trapezium and in front of the massive Orion A cloud, molecular line studies show that there are no dense cores (Bergin 1996). Hence, new stars are no longer forming in this region, and their production rate must overturn sharply. We could not resolve this rapid decline with our technique. However, one system

[1] Osservatorio Astrofisico di Arcetri, Largo Enrico Fermi 5, 50125 Florence, Italy.
[2] Department of Astronomy, 601 Campbell Hall, University of California, Berkeley, CA 94720.

from Paper II did show a decline, albeit over a longer timescale. This was Upper Scorpius, an OB association with very low gas content (de Geus, Bronfman, & Thaddeus 1990). In an interesting, related study, Dolan & Mathieu (2001) have documented the star formation history of the λ Orionis region. They found the star formation rate to be accelerating in unperturbed cloud material well removed from the massive stars, but to have fallen to a low level closer to these objects, where the gas has largely been dispersed.

The manner in which accelerating star formation ends within a low-mass T association is less clear. The results concerning λ Ori illustrate, in any case, the value of probing both the temporal and *spatial* pattern of activity. In the present paper, we apply this philosophy to the Taurus-Auriga association. This region has, of course, been thoroughly studied over many years. Stars have been cataloged through a number of deep surveys covering the optical, infrared, and X-ray regimes (Kenyon & Hartmann 1995; Briceño et al. 1998; Luhman 2000; König, Neuhäuser, & Stelzer 2001). The stellar population is located within a cloud complex that has itself been mapped systematically in a number of CO isotopes (Kawamura et al. 1998; Onishi et al. 1996; Dame, Hartmann, & Thaddeus 2001) and more sparsely in other, high-density tracers (Benson & Myers 1989; Pound & Bally 1991; Saito et al. 2001). Thus, we inherit a rich trove of data for assessing the star formation pattern.

We describe this pattern in § 2 and show how activity has become centrally concentrated with time. We then focus on those stars *outside* the central region, to confirm that they are bona fide members of the association. Section 3 discusses the implications of our findings with regard to the basic questions posed earlier. We also compare our results with recently proposed dynamical models of stellar group formation. Finally, in § 4, we indicate fruitful directions for research in the near future.

2. THE STAR FORMATION PATTERN

2.1. *Previous Studies*

The most striking aspect of the Taurus-Auriga association is the striated morphology of the parent cloud gas. This basic feature is apparent even in optical photographs of the region, as was stressed early last century by Barnard (1927). Molecular line studies, including those cited above, have since revealed the full extent of the gaseous structures. With its linear extent of 30 pc and total mass estimated at $2 \times 10^4\ M_\odot$ (Ungerechts & Thaddeus 1987), the complex nearly attains the status of a giant molecular cloud. How did this gas accumulate, and how is it producing stars today?

Gómez de Castro & Pudritz (1992) boldly addressed both questions in an interesting theoretical investigation. Using the proper-motion study of Jones & Herbig (1979), they pointed out that the young stars appear to be streaming in a direction that is parallel to that of the filaments. Gómez de Castro & Pudritz also stressed the wavelike appearance of the ambient magnetic field, which runs roughly perpendicular to the orientation of the filaments (Scalo 1990). They explained all these findings by postulating that the cloud complex formed through the magnetic Parker instability (Parker 1966). Gas flowing down buckled field lines crashes into material already in the plane, creating local concentrations of streaming gas (the dark clouds) while radiating much of the collision energy in the form of Alfvén waves. They attributed the filaments themselves to density enhancements produced by such waves when they attain mildly nonlinear amplitude. Finally, Gómez de Castro & Pudritz compared the Hα luminosity functions in two stellar groups located at opposite ends of the complex. As these functions were similar, they surmised that the complex as a whole is forming stars coevally.

More recently, a very different account was offered by Ballesteros-Paredes, Hartmann, & Vázquez-Semadeni (1999). These authors noted that the molecular gas in Taurus-Auriga is spatially correlated with H I, as seen through 21 cm surveys. Other researchers (see, e.g., Andersson & Wannier 1993) have interpreted this result as indicating the presence of an atomic envelope surrounding the molecular complex. Ballesteros-Paredes et al. emphasized that the H I line profiles are significantly broader than those of ^{12}CO, exhibit a pronounced asymmetry, and are shifted in their peak velocity. They therefore speculated that the present-day molecular filaments were created through the collision of high-speed flows in the atomic gas. The resulting dense, postshock configuration could undergo prompt gravitational collapse and initiate a burst of star formation throughout the region (see also Hartmann, Ballesteros-Paredes, & Bergin 2001).

A point not emphasized by previous authors is the spatial distribution of the stars themselves. Two facts ensure that such a study is relevant for the question of stellar birth. First, the extensive survey work by numerous researchers has now provided a nearly complete population census within the association, at least to a limiting V magnitude of 17 (Briceño et al. 1999). Note that the observational criteria here are not limited, as before, to emission-line diagnostics, so that the investigations fully account for weak-lined and post–T Tauri objects.

Apart from the completeness issue, the current positions of the stars would be of limited interest if the objects could drift far from their birth sites. However, the stars must have been born with the same velocity as the local gas. Observations indicate that this equality still holds. Specifically, the difference between stellar and cloud radial velocities is at most about 2 km s^{-1} (Hartmann et al. 1986; see also below). Even objects traveling on ballistic trajectories with this speed would cover only a few parsecs in several million years, which is the lifetime of most association members. The stellar distribution therefore does reflect conditions at birth, a point to which we return presently.

Gómez et al. (1993) pointed out that Taurus-Auriga stars are more clumped spatially than a random distribution throughout the parent clouds. Indeed, the median nearest-neighbor separation is only 0.3 pc, not much greater than the diameter of a star-forming dense core (Myers & Benson 1983). Gómez et al. identified six distinct groups, each containing about 15 individual stars or binaries, ranging in size from 0.5 to 1.0 pc. The remaining stars, some 30% of the total, have a more uniform distribution. Interestingly, Gómez de Castro & Pudritz (1992) had previously speculated that star formation in Taurus-Auriga proceeded through individual clusters. They based this idea on the observed distribution of molecular clumps, which is far more weighted to higher masses than the visible stars. Thus, if all clumps produce stars with comparable efficiency, then the most massive should yield multiple objects.

2.2. *New Findings*

We base our own investigation on a sample of 153 stars, drawn from a number of sources in the literature. Most are from the compilation of Kenyon & Hartmann (1995), who in turn utilized and supplemented earlier studies in the optical, near-infrared, and X-ray regimes. The membership list of Kenyon & Hartmann is complete to $V \sim 15$ mag. Within the L1495E cloud, both Strom & Strom (1994) and Luhman & Rieke (1998) conducted deeper surveys, which doubled the number of known members in this area. Briceño et al. (1998) focused on very low mass objects in both L1495E and other regions, uncovering nine new stars. Both the 2MASS project (Luhman 2000) and the large-scale, optical CIDA survey (Briceño et al. 1999) yielded additional objects. Finally, we have added 13 stars from the *ROSAT* study of Wichmann et al. (2000).

All told, these various sources gave us 212 member stars. Many, however, do not have published luminosities and effective temperatures, generally because they are more deeply embedded Class 0 or I sources. Those that do, a total of 153 objects, can be placed in the H-R diagram. For this subset, we were able to assign contraction ages based on our own pre–main-sequence tracks (Paper I). The zero point of these ages corresponds to the stellar birth line.[3]

Figure 1 summarizes our results for the spatial *and* temporal distribution of all 153 stars. Here, we have binned the objects into three age groups, as indicated. We have also displayed within each panel the ^{12}CO ($J = 1 \rightarrow 0$) contours of Dame et al. (2001). The lowest contour is for $\int T_A \, dV = 2$ K km s^{-1}, corresponding to a gas column density of $N_{\rm H} = 4 \times 10^{20}$ cm^{-2}, or $A_V = 0.3$ mag. Scanning the panels from left to right gives a global view of the progress of star formation throughout the entire complex.

[3] We have compiled essential data for all 212 stars in a table, available at http://www.arcetri.astro.it/~palla/taurus/table. This table includes pre–main-sequence ages for the 153 members with published luminosities and effective temperatures.

The five oldest stars in our sample all have ages of 2×10^7 yr. From this time in the past until 4 Myr ago, there were numerous stellar births, but they were widely distributed in space. On the other hand, a few discrete centers of activity are apparent even at this earliest epoch. One of the most prominent is the L1551 region, in the lower left corner of the map. Over the next 2 Myr, the original centers of activity retained their identity, but new regions began forming stars. The main characteristic of this evolution is the increase in star formation along a central group of filaments, lying along a Galactic latitude $b \approx -15°$. This concentration subsequently grew, so that the youngest stars, with ages under 2 Myr, are almost exclusively confined to the filaments. Meanwhile, the total number of objects produced per time interval, i.e., the rate of star formation, also rose. This last trend, of course, is the acceleration we found earlier (Paper II).

The central filaments represent a concentration not only of stars, but also of molecular gas. In the top panel of Figure 2, we again display, in addition to the youngest subset of stars, the ^{12}CO intensity, now over a more restricted area. We also include, through gray-scale shading, the distribution of ^{13}CO ($J = 1 \rightarrow 0$), taken from Mizuno et al. (1995). For these latter observations, the minimum detectable hydrogen column density is $N_{\rm H} = 1 \times 10^{21}$ cm^{-2}. The innermost contours, finally, display emission in C^{18}O ($J = 1 \rightarrow 0$) from Onishi et al. (1996). In this rarest of the three CO isotopes, the minimum column density is $N_{\rm H} = 4 \times 10^{21}$ cm^{-2}. It is apparent that most of the recent stellar births are occurring within, or close to, the area bright in C^{18}O. This region constitutes, in terms of column density, a narrow ridge projecting above surrounding cloud material.

Star formation within the filaments is still active at the present time. This point is made clear in the bottom panel of Figure 2. Here we reproduce the heavy contours of C^{18}O from above. We also mark the location of all NH_3 dense cores that have been found within the borders of the panel (Jijina et al. 1999). These 16 local concentrations of cloud

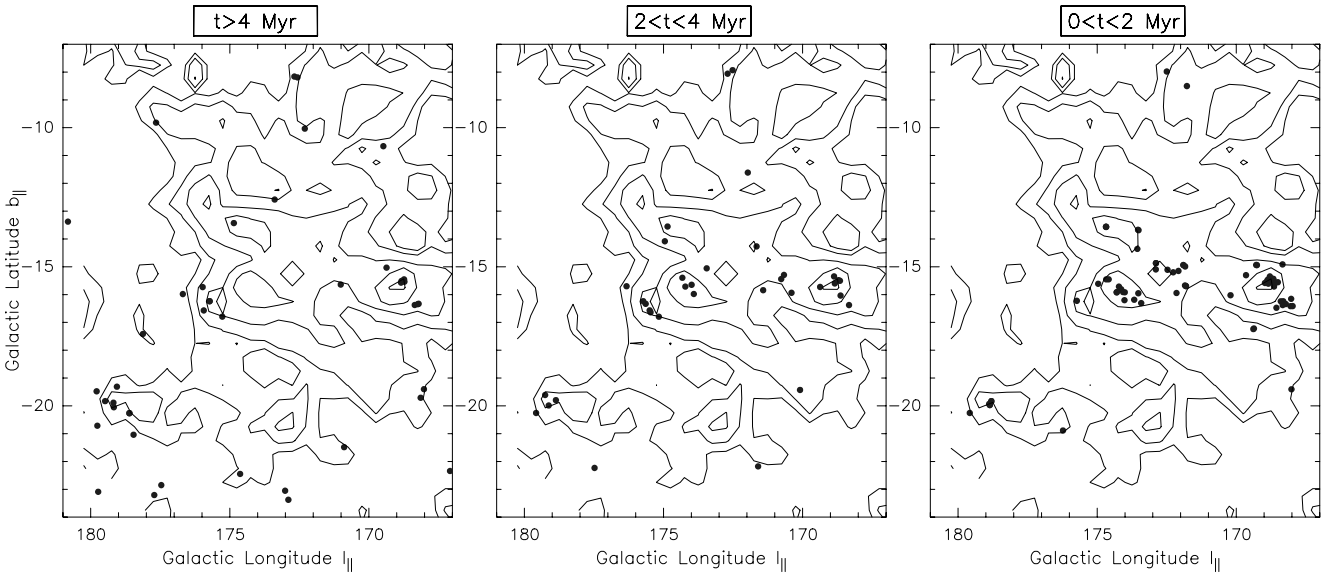

FIG. 1.—Evolution of the stellar distribution in Taurus-Auriga. Circles represent observed T Tauri stars, binned according to pre–main-sequence age, as shown. Contours represent the ^{12}CO ($J = 1 \rightarrow 0$) integrated intensity map from Dame et al. (2001).

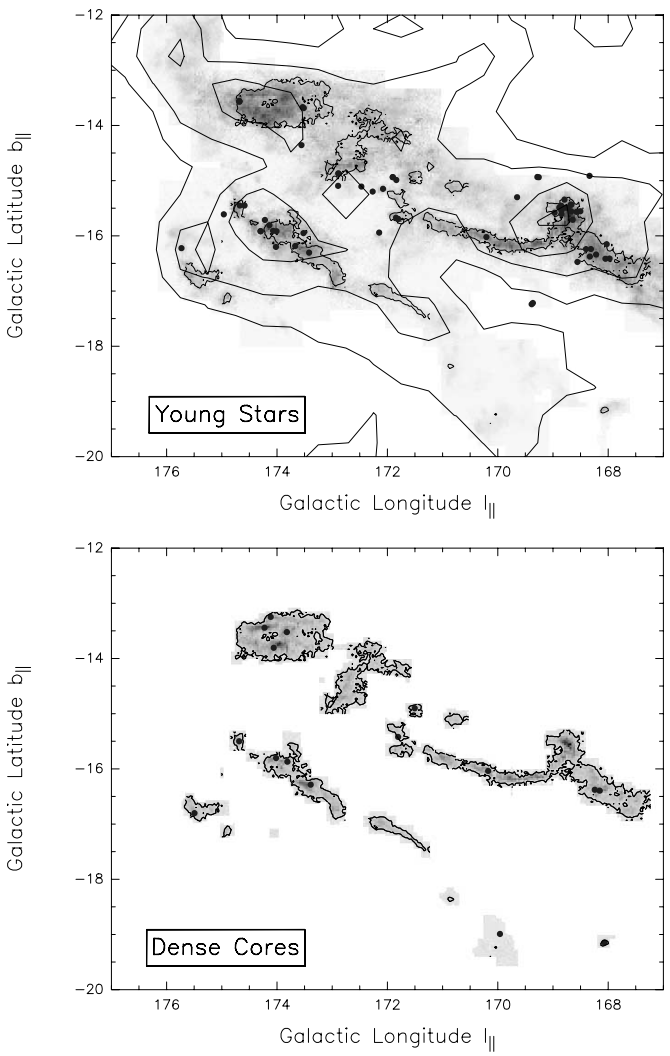

FIG. 2.—*Top*: Relation of young stars and the central filament. Dots represent T Tauri stars from the rightmost age bin of Fig. 1, and the outer contours again show the ^{12}CO integrated intensity. The gray-scale shading represents ^{13}CO ($J = 1 \rightarrow 0$) flux from Mizuno et al. (1995). Finally, the inner contours show C^{18}O ($J = 1 \rightarrow 0$) from Onishi et al. (1996). *Bottom*: Positions of NH_3 dense cores, from Jijina, Myers, & Adams (1999). Also shown is the C^{18}O emission, both as contours and in gray scale.

gas, detected through the (1, 1) inversion line, are all associated with C^{18}O emission. *IRAS* point sources are found within 10 of the objects.

It is an important characteristic of this system that the sites of individual protostar collapse are *not* scattered more widely throughout the larger parent cloud. Let us view the matter from another perspective. Both C^{18}O and NH_3 trace especially dense molecular gas. Indeed, the minimum detectable N_H for the latter is 3×10^{21} cm^{-2}. However, the critical *volume* density for excitation of NH_3 (1, 1) is 2×10^4 cm^{-3}, a factor of 5 above that for C^{18}O ($J = 1 \rightarrow 0$) (Swade 1989). Thus, while a detection of NH_3 essentially guarantees that C^{18}O will also be present, the converse is false. One can imagine a looser aggregate of NH_3 cores, each nested within an isolated patch of C^{18}O. With the exception of two objects in the lower right of Figure 2 (called L1489 and L1498), this is not the case. Most dense cores, along with the new stars they are producing, arise in a more contiguous region of enhanced density, i.e., the filaments.

Two familiar caveats that apply here concern observational selection and completeness. The surveys for dense cores examined areas already known to have a high visual extinction (see, e.g., Benson & Myers 1989) and could well have missed some objects lying outside the main concentration of cloud gas. In addition, the mapping of C^{18}O is incomplete. Could there exist other star-forming filaments within the area bounded by Figure 1? The contours of ^{12}CO that coincide presently with C^{18}O correspond to $\int T_A \, dV \gtrsim 7$ K km s^{-1}. Four other locations satisfy this criterion. These include: the L1551 cloud, centered on $l = 179°, b = -20°$; part of the Auriga region, near $l = 172°, b = -9°$; the L1544 cloud at $l = 176°, b = -10°$; and a smaller region located at $l = 173°, b = -21°$. Seventeen of our sample T Tauri stars are located in L1551, seven in the relevant part of Auriga, six in L1544, and none in the last region. In summary, while the L1551 cloud is the most conspicuous in terms of star formation activity, no region, including this one, is comparable to the main filaments.

Figure 3 compares the ages of stars located inside and outside the filaments, where the latter is defined by the C^{18}O contours. The two plots reveal strikingly different star formation histories. Activity was already present 10^7 yr ago throughout the cloud. About 3×10^6 yr ago, the rate of star formation within the larger, exterior volume reached a modest peak and subsequently fell off. Concurrently, the rate within the present C^{18}O contours attained a much higher level and continues to rise steeply today.

As we noted above, contrasting histories within adjacent regions were also recently found by Dolan & Mathieu (2001) in their study of the λ Ori association. Here, a large evacuated cavity in the ambient molecular gas surrounds the O star λ Ori. Their Figure 11 shows that low-mass star formation *outside* the cavity, i.e., in the undisturbed molecular cloud, is smoothly accelerating. Activity

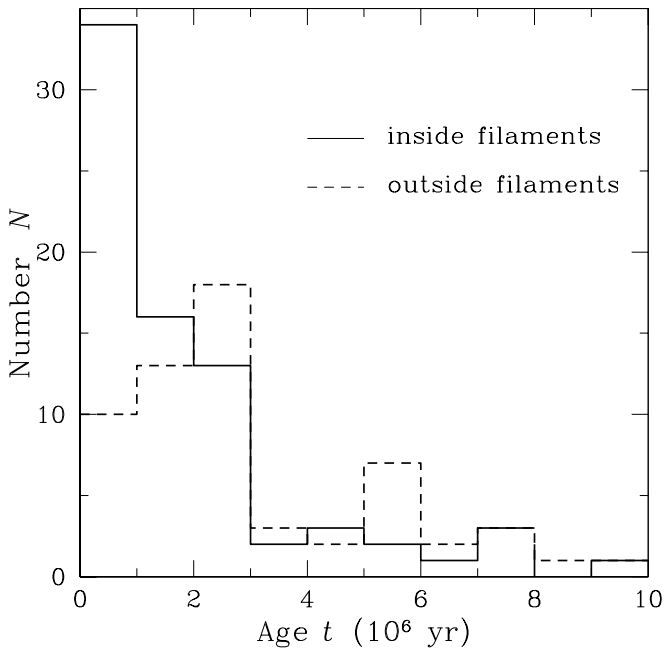

FIG. 3.—Distribution of pre–main-sequence ages for T Tauri stars inside the C^{18}O filaments of Fig. 2 (*solid histogram*). Shown for comparison (*dashed histogram*) are the ages of stars outside the filaments, but still within the ^{12}CO contours of Fig. 1.

inside the currently evacuated central region peaked about 2×10^6 yr ago, fell sharply, and has by now essentially vanished.

In the case of this OB association, the recent decline evidently results from cloud dispersal by a few massive stars. (Recall the discussion of Upper Scorpius in Paper II.) In the Taurus-Auriga T association, the decline throughout the larger volume is less steep, but might still reflect partial and ongoing dissipation, presumably through the action of low-mass stellar outflows. Both regions have vigorous star formation today wherever the parent cloud has reached *and maintained* a certain density. The recent increase in stellar births is so strong in Taurus-Auriga that it gives the impression of a *global* acceleration when all the stars in the association are tallied up (Paper II). We now see that the rising activity occurs exclusively within the central, filamentary region.

2.3. *Nature of the Outlying Stars*

Our account of star formation assumes that *all* objects in our list, including the 80 outside the $C^{18}O$ filaments but within the borders of Figure 1, are bona fide members of the association. If these outliers were instead misclassified foreground stars or interlopers from another region, then the Taurus-Auriga history would be quite different. Every object of the 153 total was classified, in the references cited earlier, as either a weak-lined or a classical T Tauri star, on the basis of Hα emission, proper motion, and radial velocity. In a few cases, lithium abundances were available as an independent check (see below). Hence, both the relative youth and membership of the outliers appears to be established.

The last point, that these pre–main-sequence stars were actually born within the confines of the present-day molecular cloud, is worth emphasizing. In Figure 4, we show the distribution of stellar radial velocity *relative* to that of the cloud. That is, we plot the difference of V_*, the stellar V_r-value, and V_{CO}, the ^{12}CO radial velocity at the same spatial location. The top panel, which refers to objects inside the filaments, shows a distribution that is largely symmetric about $V_* - V_{CO} = 0$ and extends for at least ± 2 km s^{-1} on either side. Most of this spread reflects errors in the measurement of V_*, which is less precisely determined than the gas velocity (see, e.g., Hartmann et al. 1986). Thus, the true velocity difference in each case is almost certainly less. The bottom panel, covering objects outside the filaments, reveals a similar, symmetric pattern. The outliers appear, therefore, to be physically associated with the molecular cloud.

Are the outliers, on average, older than stars inside the filaments, as Figure 3 indicates? Here a concern is the accuracy of each star's assigned luminosity and effective temperature. These values determine, via the evolutionary tracks, the pre–main-sequence contraction age. Paper II gauged the effect of unresolved binaries, while Hartmann (2001) has recently summarized other sources of error. For the luminosity, which more directly influences the age, the single biggest uncertainty arises from patchy interstellar extinction. Fortunately, the outliers are located in a region of the parent complex with relatively low column density. Figure 5 illustrates this fact by showing the distribution of the published A_V-values, again both inside and outside the filaments. It is clear that both the mean visual extinction and the maximal values are substantially lower for the outlying stars. Assuming that these are located at the same distance as other association members, their luminosities, and hence ages, should be relatively secure.

We mentioned earlier that an additional piece of evidence supporting the pre–main-sequence status of the outliers is enhanced surface lithium abundance. On the other hand, the mean age of these objects exceeds that of those inside the filaments. These two facts might seem to be in contradiction, since lithium is consumed during contraction toward

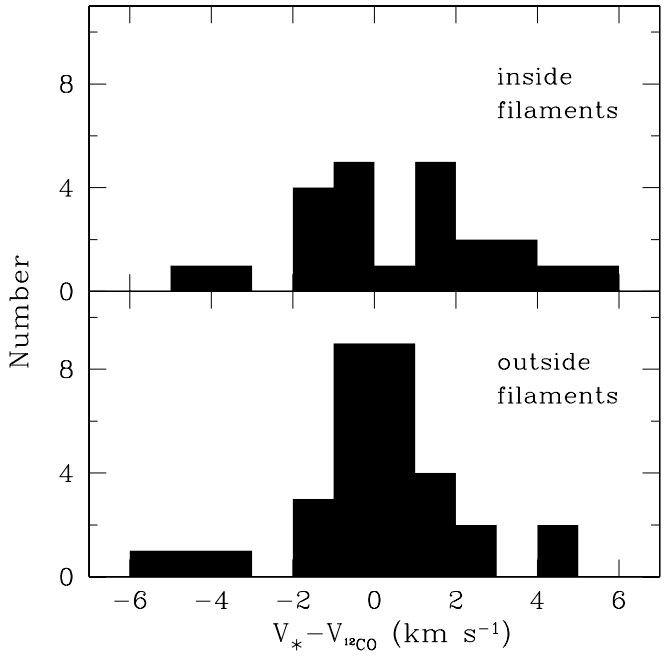

FIG. 4.—Distribution of the stellar velocity relative to the ambient cloud, for objects inside and outside the $C^{18}O$ filaments. The stellar velocity is the radial value from the optical spectrum, while the cloud velocity is that obtained in ^{12}CO ($J = 1 \rightarrow 0$).

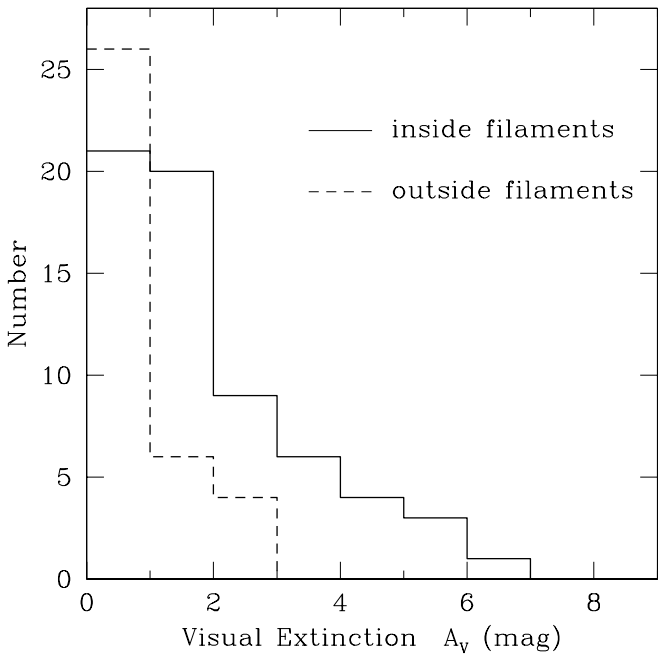

FIG. 5.—Distribution of the visual extinction A_V for stars inside (*solid histogram*) and outside (*dashed histogram*) the $C^{18}O$ filaments.

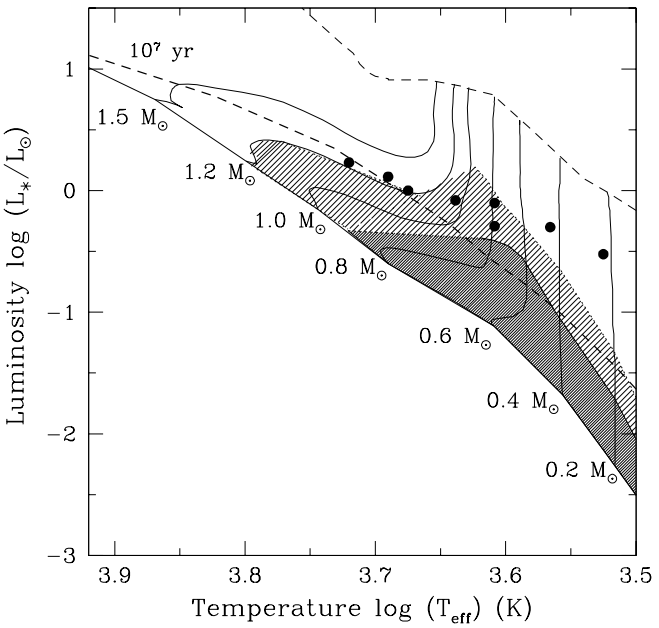

FIG. 6.—Location in the H-R diagram of all outlying stars with measured lithium abundances. The lighter shaded region represents objects in which lithium has been depleted as much as 0.1 times the interstellar value, according to Siess et al. (2000). The darker shading is for depletion greater than this amount. Shown also are pre–main-sequence tracks for the indicated mass values, in solar units, from Paper I. The dashed curves represent the birth line and the 10^7 yr isochrone.

the main sequence. The resolution here is that lithium only disappears early for stars in which the base of the convection zone exceeds the ignition temperature of 3×10^6 K (see, e.g., Siess, Dufour, & Forestini 2000).

To elaborate on this point, we display in Figure 6 the positions within the H-R diagram of the eight outliers for which we have found published lithium abundances. Objects inside the white area between the birth line and the zero-age main sequence should have the full, interstellar supply of lithium. In the lightly shaded region are objects in which the element has been depleted down to 0.1 times the interstellar value (Siess et al. 2000). Finally, the darker shading indicates depletion by more than this amount. The dashed curve is the isochrone corresponding to a contraction age of 10^7 yr.

Of the eight objects, the leftmost three are on radiative tracks and therefore should have undepleted lithium, despite ages close to 10^7 yr. The middle three are slightly younger and should have modest depletion, while the two on the right are too young for any lithium consumption. Table 1 gives the observed abundances in these objects, and each is identified as either a classical (C) or a weak-lined (W) T Tauri star. Following convention, the quantity $N(\mathrm{Li})$ in the fourth column is actually $\log(\mathrm{Li/H}) + 12$, where the argument is the number abundance of lithium relative to hydrogen. For all objects, we see that $N(\mathrm{Li})$ is either at its full, interstellar value between 2.9 and 3.2 (Zapatero Osorio et al. 2002) or is only modestly reduced.

The observational evidence is convincing that the outliers are neither interlopers from other star-forming regions nor foreground objects. They represent a portion of the Taurus-Auriga association that is more widespread than the generally younger stars within the central filaments. It is unlikely, moreover, that these objects drifted from the filaments to

TABLE 1
LITHIUM ABUNDANCES IN T TAURI OUTLIERS

Star	Type	Age (Myr)	$N(\mathrm{Li})$	Reference
GM Aur	W	9.6	3.1	1
LkCa 19	W	14.0	3.1	2
LkCa 15	C	5.2	3.1	2
V836 Tau	C	4.9	3.1	2
UX Tau A	W	8.0	3.2	2
LkCa 21	W	1.5	3.0	2
V710 Tau B	C	0.9	2.5	2
V827 Tau	W	2.5	3.2	2

REFERENCES.—(1) Magazzù, Rebolo, & Pavlenko 1992; (2) Martín et al. 1994.

their present locations. In Figure 7, we display proper-motion vectors taken from the literature (Jones & Herbig 1979; Hartmann et al. 1991; Gómez et al. 1992; Frink et al. 1997; Wichmann et al. 2000). Here we have subtracted off the mean proper motion for the central region and omitted all the resulting vectors whose magnitude is less than the typical error of 5 mas yr^{-1} (Frink et al. 1997). We see that the velocities of the outliers are *not* directed away from the $C^{18}O$ filaments, whose contours we again display.[4]

[4] The Taurus-Auriga complex appears in projection within the vast area covered by the dispersed Cas-Tau association (Blaauw 1991). One might therefore worry about contamination of our outliers by this older population. Aside from the lithium and radial velocity tests that distinguish Taurus-Auriga members, the mean proper motion of the two groups is very different in direction, so that such contamination should be minimal (de Zeeuw et al. 1999).

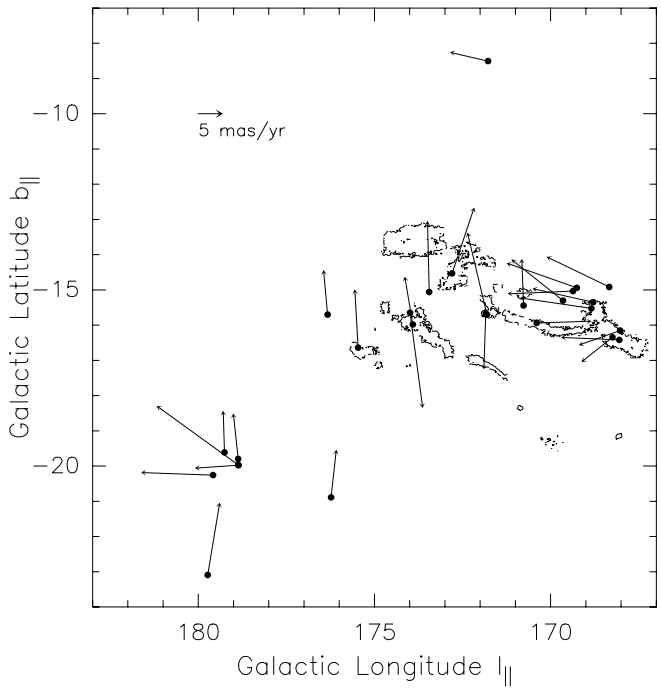

FIG. 7.—Proper motions of stars in Taurus-Auriga, as obtained from the literature. The vectors shown are the observed proper motions relative to the mean for the central filaments (Frink et al. 1997). The $C^{18}O$ outer contours are again superposed. Note that we have omitted all vectors whose magnitude, after subtraction of the mean, falls below the typical error of 5 mas yr^{-1}, which we also display.

What, then, is the significance of the observed vectors? We emphasize again that the radial motions show no substantial difference between the velocities of each star and of its local patch of molecular gas. These two velocities must have been equal just after formation of each object, and they continue to match today. The simplest interpretation of this fact is that the stars, which comprise a tiny fraction of the overall mass, have remained trapped within the local gravitational potential wells of the gas. The trapping force arises from parsec-scale regions of the complex, not individual dense cores. Such regions have their own internal motions; these appear as the vectors in Figure 7. Finally, the presence of coherent entities, such as L1544 and L1551, also attests to the fact that most stars were born in situ. Especially dense clumps have been producing stars since the earliest days of the complex.

The coexistence of a widespread and spatially concentrated population of young stars has also been documented in the L1641 region of the Orion A molecular cloud (Strom, Strom, & Merrill 1994). Of course, even the peak gas densities in the Taurus-Auriga filaments are insufficient to produce massive stars, such as those in Orion. This difference, however, might be one of degree, in a star formation pattern that is actually quite similar.

3. THEORETICAL INTERPRETATION

3.1. *Quasi-static Cloud Evolution*

Our assessment of the ages for Taurus-Auriga members demonstrates that star formation has been occurring throughout the parent cloud complex for at least 10^7 yr. This figure exceeds by an order of magnitude $t_{\rm coll}$, the time required for gravitational collapse of the associated molecular gas. The discrepancy of these two timescales is fundamental in any evolutionary model, so we should examine it with some care.

Evaluation of $t_{\rm coll}$ proceeds by first estimating the cloud density through an appropriate tracer. Such a line is ^{13}CO ($J = 1 \rightarrow 0$), which is optically thin outside the C^{18}O filaments and only marginally thick inside (Mizuno et al. 1995). Referring again to the top panel of Figure 2, we selected one representative location ($l = 170^\circ, b = -15^\circ$) outside the filaments, but within the region bright in ^{13}CO. We chose a second position ($l = 170^\circ, b = -16^\circ$) wholly within the filaments. Using spectra kindly supplied to us by A. Mizuno, we first estimated the column densities $N_{\rm H}$ in the two locations. Assuming the tracer to be optically thin, the $N_{\rm H}$-values were 2×10^{22} and 9×10^{22} cm^{-2} for the outer and inner locations, respectively. We then modeled both the ^{13}CO region and the ensemble of filaments as uniform cylinders, with radii of 2.2 and 0.35 pc, respectively. Dividing $N_{\rm H}$ by the corresponding cylinder diameters, we obtained volume densities $n_{\rm H}$. These were 1500 cm^{-3} for the outer point and 4400 cm^{-3} for the inner one. The corresponding values of $t_{\rm coll}$, taken to be $(3\pi/32G\rho)^{1/2}$, were 9×10^5 and 5×10^5 yr. For other selected exterior positions, $N_{\rm H}$ changed by at most a factor of 3, so that our $t_{\rm coll}$ is probably secure to within a factor of 2.

It is interesting to compare $t_{\rm coll}$ with the crossing time of each region. We can define $t_{\rm cross}$ as $2R/\Delta V$, where R is the cylinder radius and ΔV the line width (FWHM), as obtained from the spectra. The crossing times are then 3×10^6 and 7×10^5 yr for the outer and inner regions, respectively. While it would be inappropriate to emphasize the exact numerical values, it is apparent that $t_{\rm coll}$ and $t_{\rm cross}$ are quite similar and that both are larger in the exterior zone.[5] A rough match of these two timescales is consistent with the idea that the region in question is in force balance. That is, self-gravity is effectively opposed by an outward force manifesting itself as an enhanced, superthermal line width. This balance is also reflected in the equality of cloud *masses* derived from optically thin tracers and from the virial theorem, an equality that is seen in many systems (see, e.g., Bertoldi & McKee 1992).

The nature of the outward force is no clearer in Taurus-Auriga than in any other molecular cloud complex. The traditional view has been that turbulent motion within the strongly magnetized gas supplies the necessary support against gravity (see, e.g., McKee et al. 1993). Within the last few years, this view has been challenged, largely as a result of numerical simulations. (For a review, see Vázquez-Semadeni et al. 2000.) These studies consider a computational box filled with gas and a frozen-in magnetic field. When the fluid is agitated in a chaotic manner, opposing streams collide and produce dense formations within a crossing time. In more detail, it appears that transverse (Alfvénic) MHD waves of large amplitude become dissipative, longitudinal disturbances once they travel distances in excess of their own wavelengths (T. Hanawa 2001, private communication).

While the numerical results are clear enough, their astrophysical implications are not. The most straightforward interpretation is that all observed molecular cloud complexes must undergo prompt gravitational collapse. In the case of Taurus-Auriga, this picture is rendered untenable by the slow evolutionary timescale, as inferred from the stellar ages. Other dynamical models face a similar objection (see § 3.3 below). An alternative view is that the simulations have failed to capture the true internal motion of the gas, which is actually less chaotic and more organized. Any transverse wave, for example, apparently must have a wavelength comparable to the cloud dimension in order to survive. The motion within the cloud might be better described as a superposition of normal modes than as a broad spectrum of turbulent eddies.

Whatever its internal dynamics, any cloud destined to form stars must contract gravitationally. It is tempting to equate the inward motion with that revealed by asymmetric line profiles in various molecular tracers (Myers, Evans, & Ohashi 2000). However, these millimeter observations concern, for the most part, smaller length scales of order 0.1 pc. Olmi & Testi (2002) have recently presented evidence of cloud contraction over a size of 0.5 pc in Serpens. As these observations develop, we should bear in mind that such global cloud evolution must be mediated by energy dissipation. This loss, in turn, arises from shocks, such as those in the simulations cited above. A more ordered internal state implies that the shocks are less pervasive than in a fully turbulent medium.

[5] The crossing time would be greater if one used as a length the major axis of an individual, striated cloud. On the other hand, millimeter observations show that clumpiness persists even in the direction of greatest cloud elongation (see, e.g., Fig. 1 of Onishi et al. 1998). Our cylindrical diameters at least crudely represent the spatial scale of the largest clumping.

3.2. *Star Formation Threshold*

Despite the protracted nature of the cloud contraction, the bulk of star formation in Taurus-Auriga took place in the relatively recent past (Paper II). That is, the appearance of protostars within dense cores is localized in *time*. The main result of the present study is that this activity is also localized *spatially*, i.e., in the central filaments. These two facts are undoubtedly related. In the early phase of quasi-static evolution, few places in the cloud have contracted to the point of forming dense cores and protostars. We witness only scattered activity at isolated locales during this epoch. Eventually, contraction produces a substantial, nearly contiguous region with the requisite density to create cores. At this critical juncture, protostellar collapse occurs nearly simultaneously throughout the filaments. The spatial and temporal data, taken together, thus indicate that star formation is a *threshold* phenomenon. More precisely, this threshold refers to the conditions necessary to form multiple dense cores, which then produce stars on a relatively brief timescale.

Molecular line studies of other regions add support to this idea. Kawamura et al. (1998) conducted a large-scale survey in ^{13}CO ($J = 1 \rightarrow 0$) of the Gemini and Auriga regions. They identified 139 distinct clouds, with an average size of 3 pc. These regions are thus comparable to that mapped by the same tracer in Taurus-Auriga. Those clouds with embedded infrared sources tend to be more massive and larger. Conversely, ^{13}CO clouds without stars have masses only 30%–50% of the virial value, suggesting that they are partially confined by external pressure. The most interesting point for our discussion is the existence of a *minimum column density* for the appearance of interior stars. Kawamura et al. estimate the N_{H_2}-value as 1.6×10^{21} cm^{-2}, corresponding to $N_H = 3 \times 10^{21}$ cm^{-2}, or an A_V of 1.9 mag. A similar result was obtained for the Cepheus-Cassiopeia region by Yonekura et al. (1997). These authors find a somewhat larger threshold N_{H_2} of 2.5×10^{21} cm^{-2}.

Essentially the same conclusion can be drawn from observations of "inefficient" star formation in various complexes. Thus, the Chamaeleon star-forming region consists of three main clouds, each with a mass of order 10^4 $M_\odot$ (Mizuno et al. 2001). Two of the three clouds have embedded stars, while Chamaeleon III has neither infrared sources nor dense cores. This cloud is actually the most massive, but has the lowest peak surface density, as measured in ^{13}CO (Mizuno et al. 1998). Of the nine clouds in Lupus, only two are forming stars. These have the largest N_H-values (Hara et al. 1999).

The example of Chamaeleon III illustrates that relatively massive molecular clouds might still be barren of stars. Again, the reason is that the object has not attained sufficient density. Another example is the Coalsack, a cloud of 3500 $M_\odot$ at a distance of 180 pc. No infrared sources have been found. As described by Kato et al. (1999), the ^{13}CO is almost entirely distributed in many small cloudlets less than 0.4 pc in size, These are spread widely throughout the parent body and have an average N_{H_2} of $(1–2) \times 10^{21}$ cm^{-2}, i.e., either at or slightly below the putative threshold. The *total* molecular mass detected via ^{13}CO is only 0.2 times that in ^{12}CO, less than half the fraction in Taurus-Auriga. Thus, the Coalsack has not produced the analog of the central filaments.

3.3. *Comparison with Dynamical Models*

Our view that clouds evolve relatively slowly contrasts sharply with that advanced recently by a number of authors. In a widely cited paper, Elmegreen (2000) has claimed that the duration of star formation in molecular clouds is equivalent to one or two crossing times. Recognizing also the equality of t_{cross} and t_{coll}, Elmegreen argues that those clouds destined to form stars undergo prompt, global collapse and that this collapse in turn produces the observed stars.

The observational evidence used to support rapid star formation ranges from the age difference of Cepheid variables in the LMC to the persistence of substructure in embedded Galactic clusters. It is most appropriate to focus on the arguments based on pre–main-sequence stellar ages. Here, Elmegreen considers OB associations, such as the Orion Trapezium region. Unfortunately, these are systems in which the massive stars have already driven off the parent cloud material, so it is impossible to estimate directly either t_{cross} or t_{coll}. Even after these times have been guessed, the duration of star formation itself is problematic. As we demonstrated in Paper I, most stars within the Trapezium did form in the relatively brief interval of 2×10^6 yr. Many other stars, however, preceded them, so that activity gradually built up over at least 10^7 yr, in a manner analogous to that in Taurus-Auriga. Elmegreen correctly points out that continued equality of the stellar production and crossing timescale would lead to accelerating star formation in a contracting cloud. For now, our ignorance of the contraction history in any region prevents verification of such a claim. In the specific cases of NGC 6611 and NGC 4755, Elmegreen attributes the observed large age spreads to a series of star formation bursts. Our detailed age compilations in Paper II show no evidence of intermittent activity in the numerous other systems we examined.

Hartmann et al. (2001) have elaborated on the idea of rapid formation, supplying a more detailed physical account. In their picture, a previous episode of star formation creates an expanding shell of H I gas. The intersection of several shells compresses the gas to the point that it collapses, fragmenting simultaneously into stars over a broad front. The authors present numerical simulations, similar to those of Ballesteros-Paredes et al. (1999), to verify that shells are created in large-scale, turbulent flows.

The basic idea that new stars can be generated through the external compression of gas is well supported empirically. H I observations show the presence of supershells, hundreds of parsecs in size, that often contain stellar clusters (Yamaguchi et al. 2001; Ehlerová & Palouš 2002). On a scale smaller by an order of magnitude, one sees cloud globules both ablated and compressed by intense ultraviolet radiation. The densest portion of the globule might include embedded stars (Sugitani, Tamura, & Ogura 1995). In both examples, however, the material is impacted by previously formed *massive* stars. There is no evidence that the molecular clouds in Taurus-Auriga or other sites of low-mass star formation were created by this means. On the contrary, the morphology of the Taurus clouds, as revealed by high-resolution CO observations, bears little resemblance to either globules or expanding shells.

Even if one were to accept that molecular clouds represent swept-up and colliding shells, the notion that shell collapse produces a stellar association is ill founded. A grav-

itationally unstable slab breaks up into pieces of size comparable to the original slab thickness (Simon 1965). If one were to identify each fragment with a star, the breakup would convert essentially all the parent molecular gas into stars, in marked contrast to observations. In fact, there is no basis for such identification. Stars arise from the collapse of individual cloud cores, not parsec-scale shells or slabs. The buildup of cores prior to their collapse certainly proceeds faster in a denser cloud environment. This density enhancement might be stimulated externally, as in a supershell or irradiated globule, or it might occur internally, as in the central, contracting region of Taurus-Auriga.

4. DISCUSSION

Our investigation of Taurus-Auriga has yielded a much more detailed picture of star formation in this region than was previously available. We find that stellar births occur over a broad area until the cloud's own contraction yields a region of sufficiently high density to induce much more rapid formation. This connection between spatial and temporal trends adds further credence to our pre–main-sequence ages. It also encourages us to apply the same technique to other sites, in the hope of elucidating fundamental issues concerning stellar groups.

The Taurus-Auriga findings already give us further insight concerning the origin of such associations. Since global contraction has led to the current, active phase of stellar production, the cloud gas must have been more rarefied in the past. At that time, the surface density was everywhere below the star formation threshold. However, with only a modest decrease from the current $N_{\rm H}$-value, self-shielding would not have been effective, and the bulk of the gas would have been H I. An older study by Lucke (1978) might be pertinent in this regard. Lucke mapped the $B-V$ color excess toward many stars over a large portion of the northern sky. He surmised that the Taurus-Auriga molecular clouds are actually linked to the Perseus complex through a "supercloud" of H I gas. Whether or not such a coherent structure exists, Lucke's study reminds us that the Taurus-Auriga clouds undoubtedly appeared very different prior to the onset of star formation. The contours in the leftmost panels of our own Figure 1, which implicitly assume constancy of the cloud morphology, should therefore be viewed only as a crude schematic.

On the other major question, that of cloud dispersal and the truncation of stellar births, our study has less to contribute. Most of the 60 stars for which we have no estimates are deeply embedded and located in the central filaments. Thus, accelerating star formation will undoubtedly continue for several million years. Further progress in understanding the general issue of the cutoff will come by observing associations slightly more evolved than Taurus-Auriga, to witness firsthand expansion of the parent cloud. The discovery of TW Hydra, η Chamaeleon, and related groups is of considerable interest, but these associations are already gas-free. We note, finally, that expansion will cause the H_2 gas to become H I, in the reverse process of the prior contraction. The sighting of discrete H I clouds with embedded T Tauri and post–T Tauri stars would therefore constitute an important advance.

We are grateful to T. Dame, A. Mizuno, T. Onishi, and J. Swift for supplying us with their CO spectra and maps. In addition, R. Cesaroni, F. Massi, and L. Testi were of considerable help in the interpretation and analysis of the data. F. P. was supported throughout this project by grant ARS1/R/27/00. Funding for S. S. was through NSF grant AST 99-87266.

REFERENCES

Andersson, B.-G., & Wannier, P. G. 1993, ApJ, 402, 585
Ballesteros-Paredes, J., Hartmann, L., & Vázquez-Semadeni, E. 1999, ApJ, 527, 285
Barnard, E. E. 1927, A Photographic Atlas of Selected Regions of the Milky Way (Washington: Carnegie Inst.)
Benson, P. J., & Myers, P. C. 1989, ApJS, 71, 89
Bergin, T. 1996, Ph.D. thesis, Univ. Massachusetts
Bertoldi, F., & McKee, C. F. 1992, ApJ, 395, 140
Blaauw, A. 1991, in The Physics of Star Formation and Early Stellar Evolution, ed. C. J. Lada & N. D. Kylafis (Dordrecht: Kluwer), 125
Briceño, C., Calvet, N., Kenyon, S., & Hartmann, L. 1999, AJ, 118, 1354
Briceño, C., Hartmann, L., Stauffer, J., & Martín, E. L. 1998, AJ, 115, 2074
Dame, T. M., Hartmann, D., & Thaddeus, P. 2001, ApJ, 547, 792
de Geus, E. J., Bronfman, L., & Thaddeus, P. 1990, A&A, 231, 137
de Zeeuw, P. T., Hoogerwerf, R., de Bruijne, J. H. J., Brown, A. G. A., & Blaauw, A. 1999, AJ, 117, 354
Dolan, C. J., & Mathieu, R. D. 2001, AJ, 121, 2124
Ehlerová, S., & Palouš, J. 2002, MNRAS, 330, 1022
Elmegreen, B. G. 2000, ApJ, 530, 277
Frink, S., Röser, S., Neuhäuser, R., & Sterzik, M. F. 1997, A&A, 325, 613
Gómez, M., Hartmann, L., Kenyon, S. J., & Hewitt, R. 1993, AJ, 105, 1927
Gómez, M., Jones, B. F., Hartmann, L., Kenyon, S. J., Stauffer, S. J., Hewett, R., & Reid, I. N. 1992, AJ, 104, 762
Gómez de Castro, A. I., & Pudritz, R. E. 1992, ApJ, 395, 501
Hara, A., Tachihara, K., Mizuno, A., Onishi, T., Kawamura, A., Obayashi, A., & Fukui, Y. 1999, PASJ, 51, 895
Hartmann, L. 2001, AJ, 121, 1030
Hartmann, L., Ballesteros-Paredes, J., & Bergin, E. A. 2001, ApJ, 562, 852
Hartmann, L., Hewett, R., Stahler, S. W., & Mathieu, R. D. 1986, ApJ, 309, 275
Hartmann, L., Jones, B. F., Stauffer, J. R., & Kenyon, S. J. 1991, AJ, 101, 1050
Hillenbrand, L. A. 1997, AJ, 113, 1733
Jijina, J., Myers, P. C., & Adams, F. C. 1999, ApJS, 125, 161
Jones, B. F., & Herbig, G. H. 1979, AJ, 84, 1872
Kato, S., Mizuno, N., Asayama, S., Mizuno, A., Ogawa, H., & Fukui, Y. 1999, PASJ, 51, 883
Kawamura, A., Onishi, T., Yonekura, Y., Dobashi, K., Mizuno, A., Ogawa, H., & Fukui, Y. 1998, ApJS, 117, 387
Kenyon, S. J., & Hartmann, L. 1995, ApJS, 101, 117
König, B., Neuhäuser, R., & Stelzer, B. 2001, A&A, 369, 971
Lucke, P. B. 1978, A&A, 64, 367
Luhman, K. L. 2000, ApJ, 544, 1044
Luhman, K. L., & Rieke, G. H. 1998, ApJ, 497, 354
Magazzù, A., Rebolo, R., & Pavlenko, Y. V. 1992, ApJ, 392, 159
Martín, E. L., Rebolo, R., Magazzù, A., & Pavlenko, Y. V. 1994, A&A, 282, 503
McKee, C. F., Zweibel, E. G., Goodman, A. A., & Heiles, C. 1993, in Protostars and Planets III, ed. E. H. Levy & J. I. Lunine (Tucson: Univ. Arizona Press), 327
Mizuno, A., Onishi, T., Yonekura, Y., Nagahama, T., Ogawa, H., & Fukui, Y. 1995, ApJ, 445, L161
Mizuno, A., Yamaguchi, R., Tachihara, K., Toyoda, S., Aoyama, H., Yamamoto, H., Onishi, T., & Fukui, Y. 2001, PASJ, 53, 1071
Mizuno, A., et al. 1998, ApJ, 507, L83
Myers, P. C., & Benson, P. J. 1983, ApJ, 266, 309
Myers, P. C., Evans, N. J., II, & Ohashi, N. 2000, in Protostars and Planets IV, ed. V. Mannings, A. P. Boss, & S. S. Russell (Tucson: Univ. Arizona Press), 217
Olmi, L., & Testi, L. 2002, A&A, 392, 1053
Onishi, T., Mizuno, A., Kawamura, A., Ogawa, H., & Fukui, Y. 1996, ApJ, 465, 815
———. 1998, ApJ, 502, 296
Palla, F., & Stahler, S. W. 1990, ApJ, 360, L47
———. 1999, ApJ, 525, 772 (Paper I)
———. 2000, ApJ, 540, 255 (Paper II)
Parker, E. N. 1966, ApJ, 145, 811
Pound, M. W., & Bally, J. 1991, ApJ, 383, 705
Saito, M., Kawabe, R., Kitamura, Y., & Sunada, K. 2001, ApJ, 547, 840
Scalo, J. 1990, in Physical Processes in Fragmentation and Star Formation, ed. R. Capuzzo-Dolcetta, C. Chiosi, & A. di Fazio (Dordrecht: Kluwer), 151
Siess, L., Dufour, E., & Forestini, M. 2000, A&A, 358, 593
Simon, R. 1965, Ann. d'Astrophys., 28, 40

Strom, K. M., & Strom, S. E. 1994, ApJ, 424, 237
Strom, K. M., Strom, S. E., & Merrill, K. M. 1993, ApJ, 412, 233
Sugitani, K., Tamura, M., & Ogura, K. 1995, ApJ, 455, L39
Swade, D. A. 1989, ApJ, 345, 828
Ungerechts, H., & Thaddeus, P. 1987, ApJS, 63, 645
Vázquez-Semadeni, E., Ostriker, E. C., Passot, T., Gammie, C. F., & Stone, J. M. 2000, in Protostars and Planets IV, ed. V. Mannings, A. P. Boss, & S. S. Russell (Tucson: Univ. Arizona Press), 3
Wichmann, R., et al. 2000, A&A, 359, 181
Yamaguchi, R., Mizuno, N., Onishi, T., Mizuno, A., & Fukui, Y. 2001, PASJ, 53, 959
Yonekura, Y., Dobashi, K., Mizuno, A., Ogawa, H., & Fukui, Y. 1997, ApJS, 110, 21
Zapatero Osorio, M. R., Béjar, V. J. S., Pavlenko, Y. V., Rebolo, R., Allende Prieto, C., Martín, E. L., & García López, R. J. 2002, A&A, 384, 937